Septate Junctions in Imaginal Disks of *Drosophila*: A Model for the Redistribution of Septa during Cell Rearrangement

DIANNE K. FRISTROM
Department of Genetics, University of California, Berkeley, California 94720

ABSTRACT The organization of septate junctions during morphogenesis of imaginal disks is described from freeze-fracture replicas and thin sections with a view to understanding junction modulation during rearrangements of cells in epithelia. The septate junctions of each epithelial cell of the disk are distributed in a number of discrete domains equal to the number of neighboring cells. Individual septa traverse domains of contact between pairs of adjacent cells, turn downwards at the lateral boundary of the domain and run parallel to the intersection with a third cell. This arrangement leaves small channels at three-cell intersections that are occupied by specialized structures termed "tricellular plugs." Cell rearrangement involves a progressive change in the width of contact domains between adjacent cells, until old contacts are broken and new ones established. It is proposed that the septate junction adjusts to the changing width of domains by the compaction or extension of existing septa. This redistribution of septa theoretically allows a transepithelial barrier to be maintained during cell rearrangements. The applicability of this model to other epithelial tissues is discussed.

The morphogenesis of an epithelium has previously been assumed to be limited to movements of entire epithelial sheets, with each cell within the epithelium retaining its immediate neighbors (1, 2). The presence of specialized connections between adjacent epithelial cells and the absence of morphological evidence of locomotion undoubtedly contributed to this view. However, rearrangements of cells (i.e., cell movements involving change of neighbors within a contiguous epithelial sheet) have recently been described during the evagination of imaginal disks in *Drosophila* (3, 4), neurulation in newts (5), gastrulation in *Xenopus* (6), regeneration in *Hydra* (7), and epiboly in teleosts (8). Thus, cell rearrangement appears to be a widespread phenomenon in epithelial morphogenesis.

In most of the examples cited above, intercellular junctions persist during cell rearrangement (3, 6–8). Because junctions are sites of intercellular adhesion between pairs of adjacent cells, the exchange of neighbors requires some form of junction modulation (9). Tight junctions of vertebrates and septate junctions of invertebrates present particularly formidable barriers to cell rearrangement because they bridge or close off the intercellular space between a given cell and all of its neighbors, ensuring contiguity of the epithelial layer and providing a barrier to the extracellular movement of molecules across the epithelium (10–12). Thus, each cell *appears* to be fixed with respect to its neighbors.

This paper focuses on the distribution of septa and the potentially dynamic organization of the septate junction during cell rearrangement in imaginal disks. The detailed structure of the septate junction is well known. Rows of septa connect adjacent cells and separate the apical from the basal intercellular space. The plasma membranes on both sides of a septum contain rows of intramembrane particles that follow the course of the septum (13, 14). The overall arrangement of the septate junction is less well known. It is generally envisioned as a girdle encircling the periphery of cells. However, Noirot-Timothée and Noirot (15) have shown that this is not the case in the adult gut epithelium of several insects. Instead, individual septa connect pairs of adjacent cells and, at the intersection with a third cell, turn basally and run parallel to the intersection until they terminate. Thus, rather than forming a continuous band around the cell, the septa are distributed in a series of discrete domains equal to the number of neighboring cells. The present work shows that a similar arrangement of the septate junction is present in an undifferentiated tissue, the imaginal disks of *Drosophila*, and persists as the disks undergo cell rearrangements. A model for cell rearrangement is proposed in which septa are redistributed within their domains such that a transepithelial barrier can be maintained without requiring rapid breakdown and reformation of septate components. Observations in the literature are discussed that suggest that the ar-

THE JOURNAL OF CELL BIOLOGY · VOLUME 94 JULY 1982 77-87

rangement described here may apply to septate junctions in general. Parallels between septate and tight junction organization are also discussed.

MATERIALS AND METHODS

Freeze-fracture

In order to have a convenient volume of tissue for fracturing, disks isolated en masse (16) were used. Mass-isolated disks from late third instar larvae evaginate in vitro in response to 20-hydroxyecdysone and appear ultrastructurally identical to disks that undergo morphogenesis in vivo (3). Observations were made on unevaginated, partially evaginated, and fully evaginated disks by incubating mass-isolated disks in Robb's medium (17) with 0.1 μg/ml 20-hydroxyecdysone for 0, 9, and 21 h. Controls were incubated for 0, 9, and 21 h in Robb's medium without hormone. Mass-isolated disks from mid-third instar larvae (i.e., disks that had never been exposed to the high titers of hormone found at puparium formation) were also prepared. After incubation, the disks were fixed for 30 min in 1% glutaraldehyde in 0.05 M sodium cacodylate, rinsed twice in 0.1 M sodium cacodylate, and soaked overnight in 30% glycerol in 0.1 M sodium cacodylate.

Mass-isolated disks were also induced to undergo accelerated evagination (18) by treatment with 0.1% trypsin (Sigma Chemical Co., St. Louis, MO., twice crystallized) in Robb's medium, after a 7-h exposure to 0.1 μg/ml 20-hydroxyecdysone. Trypsinization was stopped after 10 min by the addition of 1% soybean trypsin inhibitor, and the disks were prepared as described above. The fixed, glycerinated disks were piled onto 3-mm cardboard circles and frozen rapidly in Freon 22 over liquid nitrogen. Freeze-fracturing was carried out in a Balzers BA 360M (Hudson, NH).

Thin Sections

Disks were fixed in 2% glutaraldehyde, 0.5% paraformaldehyde in 0.75 M sodium cacodylate buffer, postfixed in 2% OsO_4, and embedded in Polybed. Sections were stained with uranyl acetate and lead citrate and examined in a JEOL JEM 100CX electron microscope.

RESULTS

Background

Imaginal disks are larval epithelial structures that give rise to most of the external structures of the fly. During metamorphosis, disks destined to form appendages undergo a dramatic change in shape. The morphogenesis of a leg disk is shown schematically in Fig. 1 *a*. The basic change in shape of the disk is produced by an elongation and narrowing of the tissue, a process referred to as evagination. Evagination, in turn, is accomplished largely by the rearrangement of cells within the single-cell-thick epithelium, such that the number of cells in the long axis increases while the number of cells encircling the disk decreases (Fig. 1 *b*). Thus, small movements of many cells result in an exchange of neighboring cells and a change in shape of the tissue (4). Rearrangement appears to be accomplished by the active movement of the disk cells themselves rather than as a passive response to external forces (19). The kinetics of such movements are clearly important in distinguishing between the possible mechanisms of rearrangements and the mechanisms by which junctional connections permit and/or assist neighbor exchanges. While we do not yet know the rates of movements of individual cells, it is important to note that the in vitro evagination of disks can be greatly accelerated by the presence of 0.1% trypsin (18) so that a considerable change in shape of the tissue occurs within 10 min, instead of hours.

The Organization of the Septate Junction in Disks

The septate junction of imaginal disks is of the pleated sheet type (20). In freeze-fracture replicas, long, winding, multistranded rows of intramembrane particles mark the course of individual septa. The particles appear on the P (protoplasmic) face (Fig. 2), that half of the surface bilayer adjacent to the cytoplasm (21). In some regions, faint indications of complementary grooves or pits can be seen on the E (external) face (Fig. 2). The basic organization of the septate junction was similar in all stages of evagination observed, including accelerated evagination in the presence of trypsin.

Conclusions concerning the three-dimensional distribution of septa in disks were largely inferred from the pattern of distribution of intramembrane septate particles in freeze-fracture replicas. Because the disk epithelium is only a single cell thick and the cell diameter is small (5–10 μm), the fracture plane frequently passes through the surface bilayer of a series of adjacent cells. It is possible to identify the position of three-cell intersections in such fractures even though the surface of only one of the cells contributing to the intersection can usually be seen. A cell usually forms an angle or corner where it meets two adjacent cells. A change in angle of the surface with respect to the source of the shadowing material results in a difference in density of the shadow. Thus, places where three cells meet are usually marked by an abrupt change in shadow density (e.g., Figs. 3 and 4). Diagrammatic insets in Figs. 3–5 show the neighbor relationships of the fractured cells in a plane projected

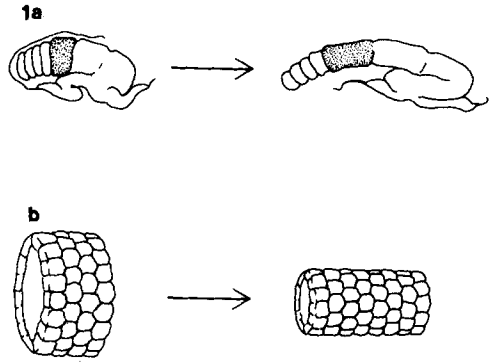

FIGURE 1 Leg disk evagination. (*a*) The transition from a partly to a fully evaginated leg disk. The first tarsal segment is stippled. (*b*) Schematic representation of the first tarsal segment. Note that the change in shape of the segment is related to a change in arrangement of cells (i.e., the number of cells in the long axis increases as the number of cells encircling the segment decreases).

FIGURE 2 A freeze-fracture micrograph of a disk incubated for 21 h in 20-hydroxyecdysone. *Pf*, protoplasmic face; *Ef*, external face; black arrows, rows of P-face septate particles and complementary E-face grooves; white arrows, E-face particles following a three-cell intersection; *g*, gap junctions. × 64,000.

FIGURE 3 A freeze-fracture micrograph from a mid-third instar disk showing an intersection between three cells, *A*, *B*, and *C*. *Inset* shows the path of the fracture plane (dashed line) through the surface bilayer of the three cells projected at right angles to an imaginary line between the asterisks. Black arrows, rows of septate particles on the protoplasmic face (*Pf*); white arrow, a row of particles on the external face (*Ef*); *as*, apical surface; *is*, intercellular space. × 40,000.

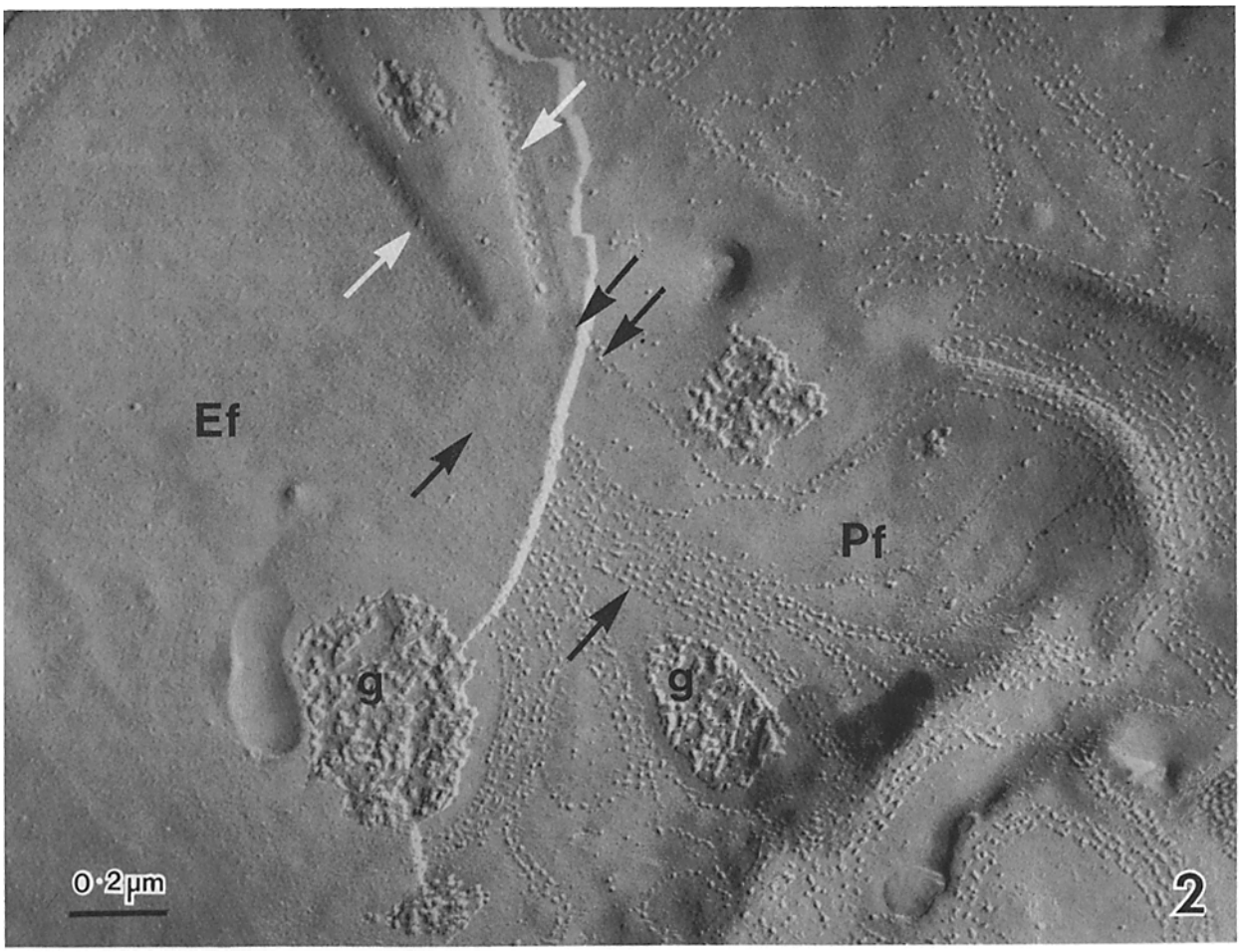
Ef
Pf
g
g
0·2 µm
2

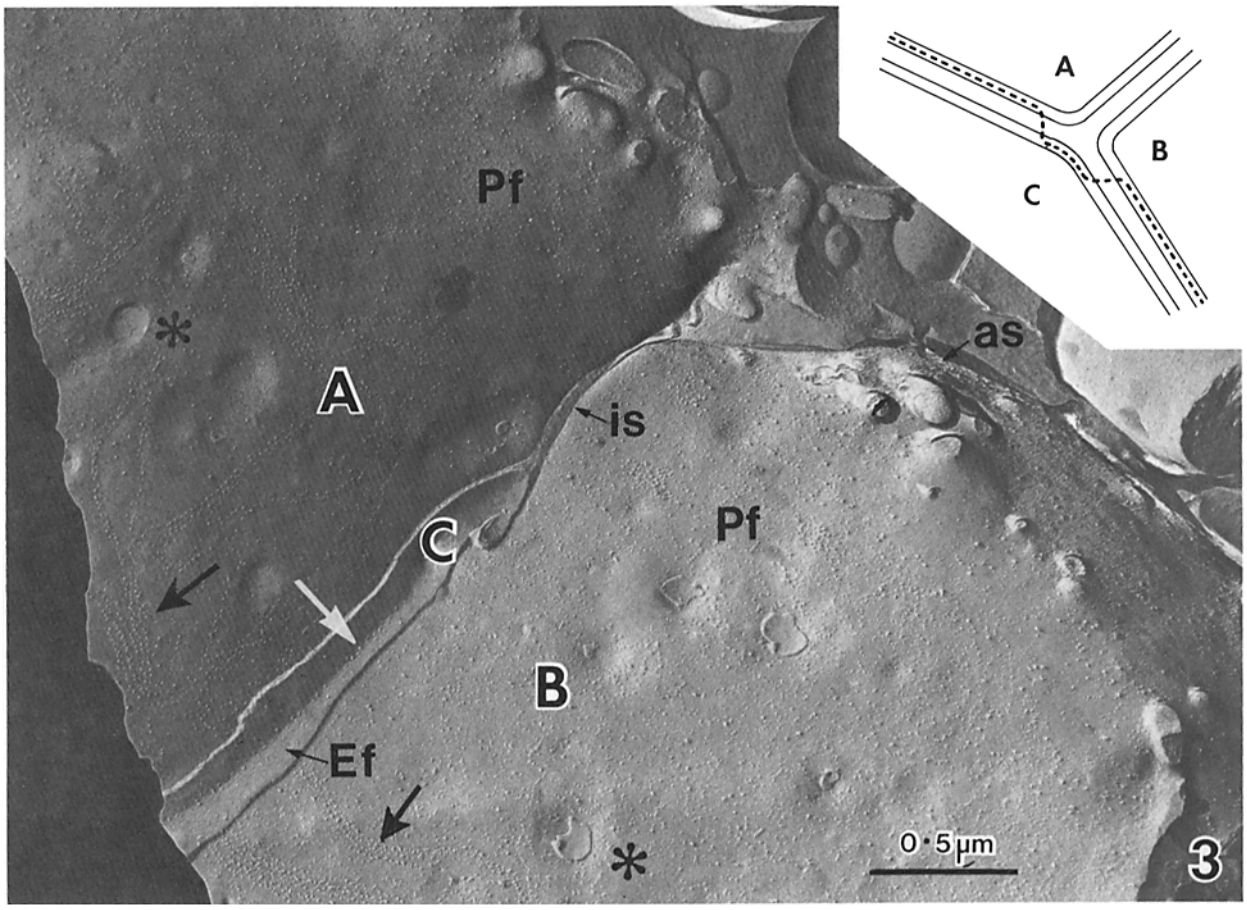
A
B
C
Pf
as
is
A
C
Pf
B
Ef
0·5 µm
3

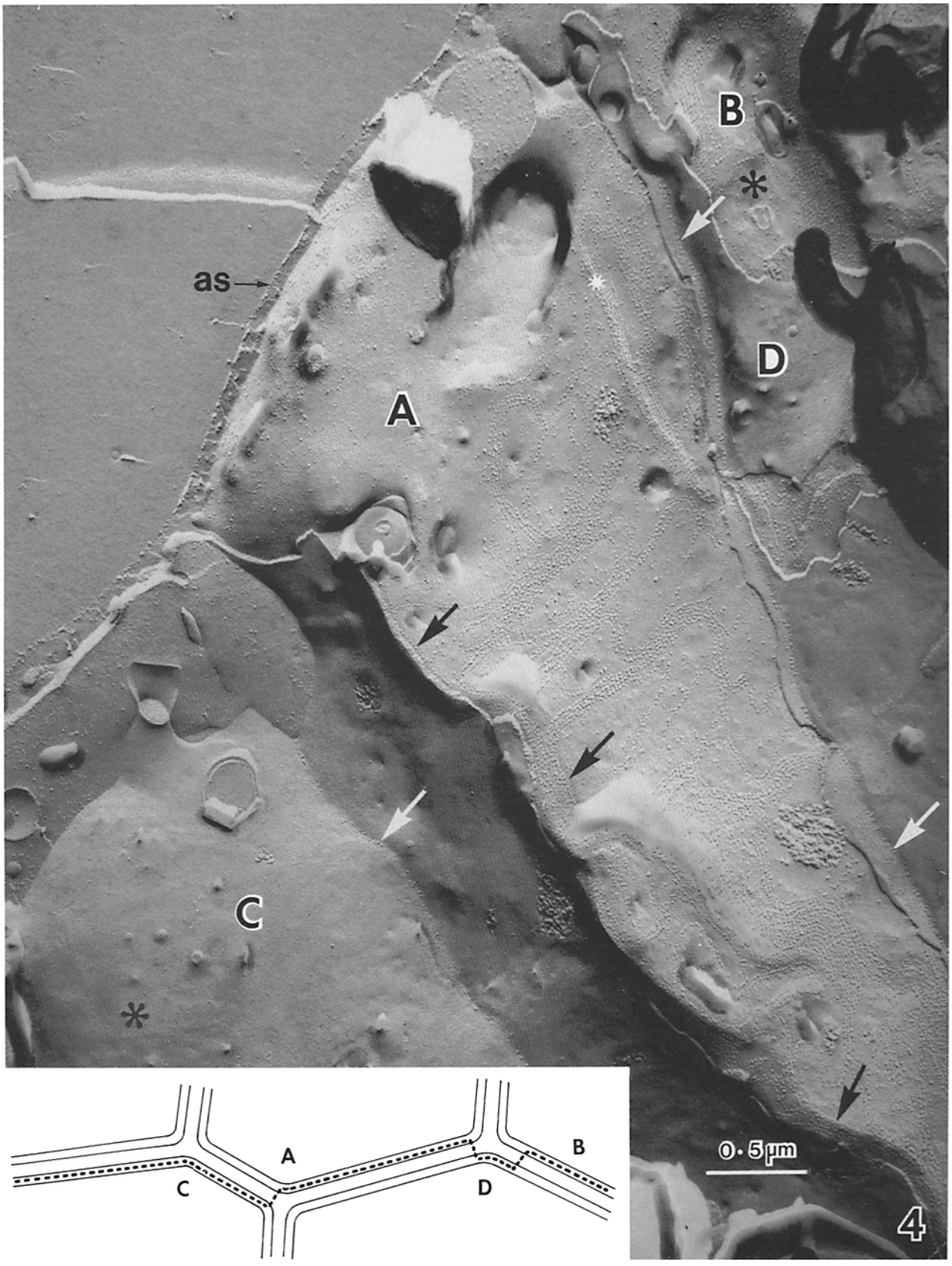

FIGURE 4 A freeze-fracture micrograph from a disk incubated for 21 h in 20-hydroxyecdysone. The fracture plane passes through the surface of four cells (*A–D*) and three three-cell intersections. *Inset* as in Fig. 3. Black arrows, rows of P-face particles parallel to three-cell intersections; white arrows, rows of E-face particles along three-cell intersections; *as*, apical surface with a layer of epicuticle. See text for further explanation. × 36,000.

FIGURE 5 A freeze-fracture micrograph from a disk incubated for 21 h in 20-hydroxyecdysone. The fracture plane passes through six cells (*A–F*) and five three-cell intersections. *Inset* as in Fig. 3. Note the P-face particles running parallel to the three-cell intersections, especially where cells interdigitate (black arrows). Otherwise, as for Figs. 3 and 4. White asterisk is explained in text. × 30,000.

at right angles to the plane of the replica. For example, in Fig. 3, the fracture plane reveals the P face of the two adjacent cells (*A* and *B*). At the apical ends of these cells, the fracture plane passes across the intercellular space. More basally, the fracture plane skips to the E face of a third cell (*C*) which forms a three-cell intersection with *A* and *B*. Bear in mind that the P face represents the inner half of the plasma membrane of a cell situated *below* the plane of the micrograph, whereas the E face represents the outer half of the plasma membrane of a cell *above* the plane of the micrograph. More complex arrangements showing a number of three-cell intersections in the same micrograph are shown in Figs. 4 and 5.

As the rows of P-face septate particles approach a three-cell intersection, they turn sharply downwards and run close to and parallel to the intersection until they terminate or occasionally loop back across the cell (Figs. 4 and 5). Typically, one or two or as many as eight rows of particles may run parallel to a three-cell intersection at any given point. Because there is good evidence that the rows of P-face particles correspond to the position of intercellular septa (13, 14), one can conclude that individual septa approach but never cross a three-cell intersection. When septa meet an intersection they turn abruptly towards the basal surface and run close to and parallel to the lateral cell boundary, as shown schematically in Fig. 6. Thin sections cut parallel to the apical surface of the epithelium show transversely sectioned septa near three-cell intersections (Fig. 7), supporting this interpretation.

This arrangement of septa leaves potentially "leaky" channels at three-cell intersections. However, it appears that in the region of the septate junction such channels are occupied by a highly specialized structure consisting of a stack of closely spaced lens-shaped plates or diaphragms. Because these structures probably contribute to the permeability barrier they will be referred to as tricellular plugs. First described in 1980 by Noirot-Timothée and Noirot (15) and now identified in imaginal disks (Fig. 8), tricellular plugs are probably a common component of the septate junction (see Discussion). It seems surprising that such a distinctive junctional structure has only been recently recognized. However, it is apparent from the longitudinal section of a tricellular plug shown in Fig. 8 that these structures are superficially very similar to the familiar ladderlike arrays of transversely sectioned septa and have probably been mistaken as such by many workers. The following criteria can be used to distinguish longitudinal sections of tricellular plugs from transversely sectioned septa. First, the diaphragms appear to be shaped like hollow lenses rather than like dense bars. Second, they are closely and regularly spaced over much longer distances than are the transversely sectioned septa (Fig. 8 *a*). Finally, a positive identification of a tricellular plug can be made in regions where the ladderlike array can be seen immediately adjacent to rows of pleated sheets (Fig. 8 *a* and *b*). Given that septa do not cross three-cell intersections, it is impossible to have transversely sectioned septa ("ladders") adjacent to longitudinally sectioned septa (pleated sheets) without any intervening plasma membrane. Thus, the "ladders" in this type of configuration cannot represent transversely sectioned septa and are interpreted as the diaphragms of a tricellular plug.

The periodicity of the alternate apices of the pleated sheets appear to correspond to the spacing of the diaphragms in the tricellular plug (20 nm). Indeed, in the high-resolution micrographs of Noirot-Timothée and Noirot (15), it appears that the diaphragms are structurally connected to the apices of the adjacent pleated sheet. Tricellular plugs are not well resolved in transverse sections of three-cell intersections (see inset Fig. 7), no doubt because of the close spacing of the diaphragms (20 nm) relative to section thickness (80 nm).

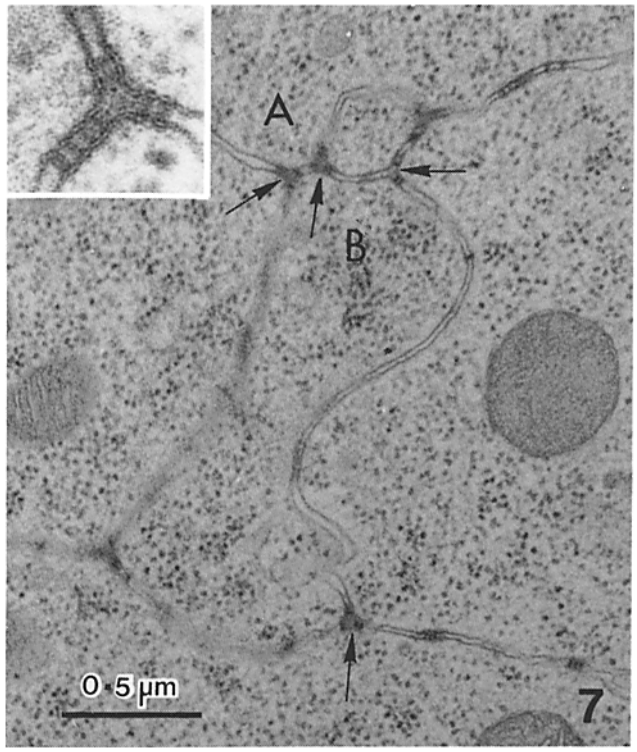

FIGURE 7 A thin section showing a number of three-cell intersections with transversely sectioned septa (arrows). Note that only two septa connect cells *A* and *B* in the plane of the section. × 36,000. *Inset,* a transversely sectioned three-cell intersection. × 100,000.

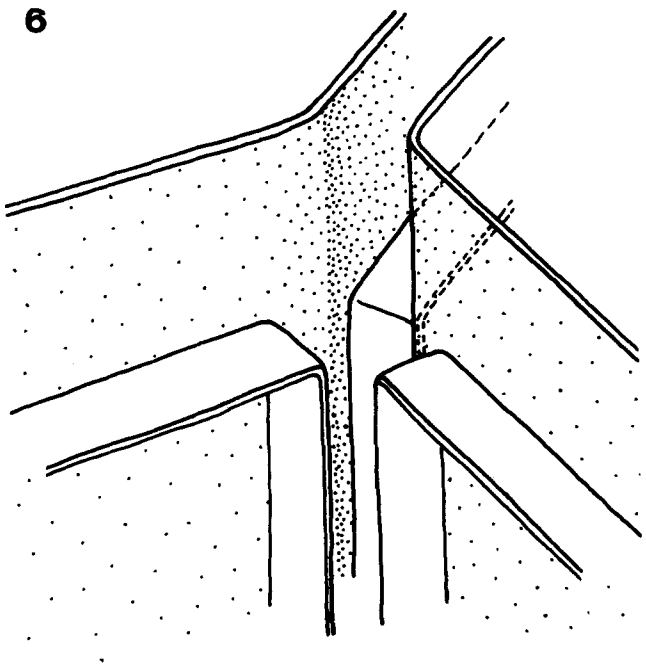

FIGURE 6 Diagram showing the arrangement of septa at a three-cell intersection. For simplicity, the septa are shown as straight rather than pleated.

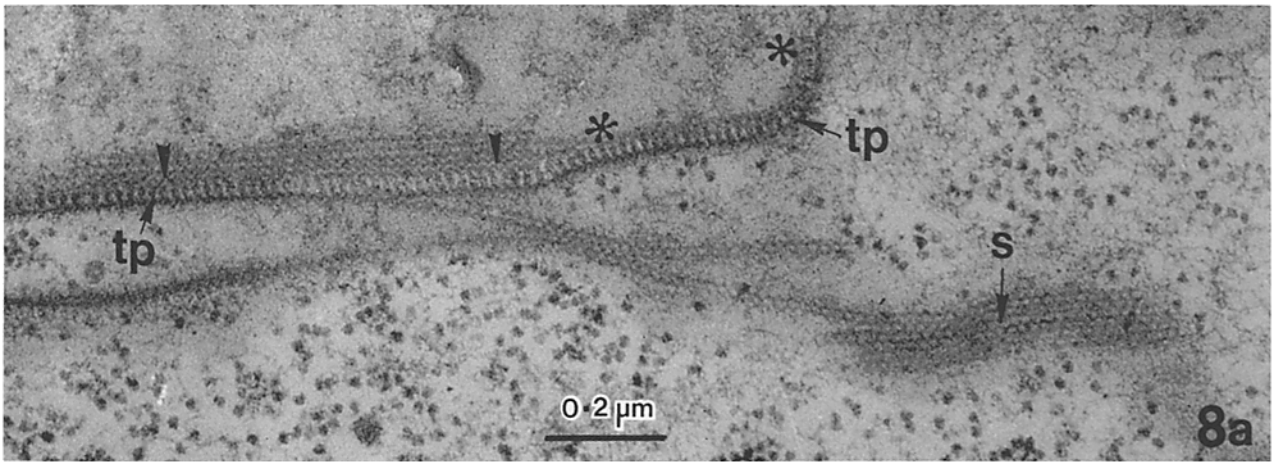

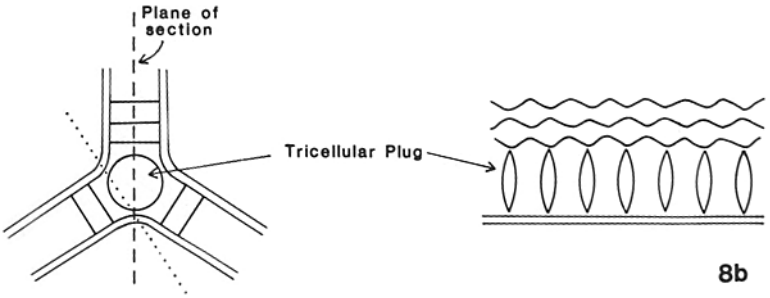

FIGURE 8 (*a*) A thin section showing a tricellula plug (*tp*) composed of an evenly spaced stack of diaphragms. The section also shows septa (*s*) sectioned longitudinally. Note that the septa adjacent to the tricellular plug (arrowheads) are oriented perpendicular to the diaphragms of the plug. × 80,000. See *b* for further explanation. (*b*) Schematic interpretation of *a*. A section cut through a three-cell intersection in the direction indicated by the dashed line (left) might reveal a structure such as seen between the arrowheads in *a*, where the diapnragms of the tricellular plug are bounded above by longitudinally sectioned septa and below by a plasma membrane. This arrangement is shown schematically at right. However, if the plane of section passes through the intersection but not through one of the three lateral sets of septa (as indicated by the dotted line at left), one might obtain the image seen between the asterisks in *a*, where the diaphragms of the plug are bounded on both sides by plasma membrane. Note that section thickness is about twice the width of the intercellular space.

The distribution of intramembrane P-face particles associated with the intercellular septa is described above. The E face, in contrast, is largely devoid of particles except for single rows at three-cell intersections. These E-face rows lie precisely along the angle of flexion at cell corners (white arrows in Figs. 2–5) and are aligned with the lateral regions of the P-face rows (Fig. 2). The E-face particles are similar in size to the P-face particles but are more irregularly arranged. Gaps in the E-face rows may be due to loss of particles during preparation or adherence of some particles to the P face. Such particle rows do not appear to be associated with septa since septa do not connect cells exactly at the corner but a short distance back (Fig. 7). It is more likely that the E-face rows are associated with the diaphragms of the tricellular plugs, as suggested by Noirot-Timothée and Noirot (15).

In summary, the septate junction appears to be composed of two sets of components, illustrated schematically in Fig. 9. There are the familiar rows of P-face intramembrane particles and intercellular septa that connect pairs of adjacent cells and the recently recognized E-face particles and tricellular plugs found at three-cell intersections.

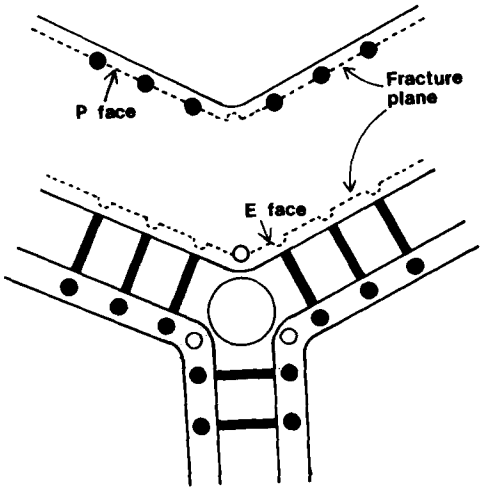

FIGURE 9 Schematic representation of the components of the septate junction at a three-cell intersection. Intercellular septa and associated P-face particles are shown in black; the tricellular plug and associated E-face particles in open circles.

The Dynamics of Septate Junction Organization: A Model for the Redistribution of Septa during Cell Rearrangement

The arrangement of septate components described above persists throughout the evagination of imaginal disks, a process involving extensive cell rearrangements (4). The time course of evagination can be accelerated at least 10-fold in the presence of trypsin (18). The characteristic structure of the septate junction persists in trypsin-accelerated disks. Freeze-fracture micrographs show the typical distribution of P- and E-face particles (Fig. 10 *a* and *b*), and thin sections show intercellular septa and tricellular plugs (Fig. 11). Considering the speed with which neighbor exchanges must occur in the presence of trypsin, it is difficult to imagine that the septate junction could break down and re-form without leaving evidence for such a process at the ultrastructural level (12, 22).

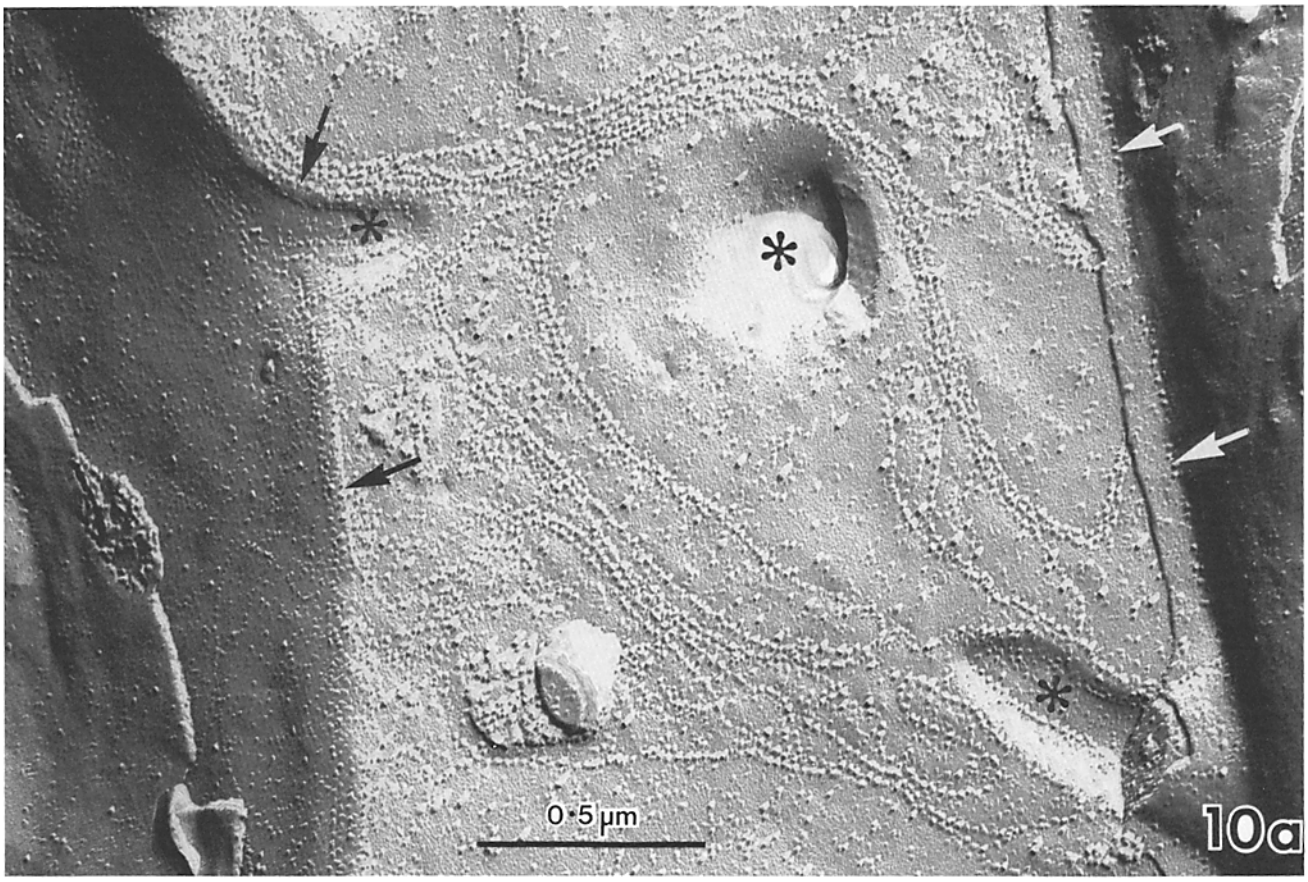
0·5 µm
10a

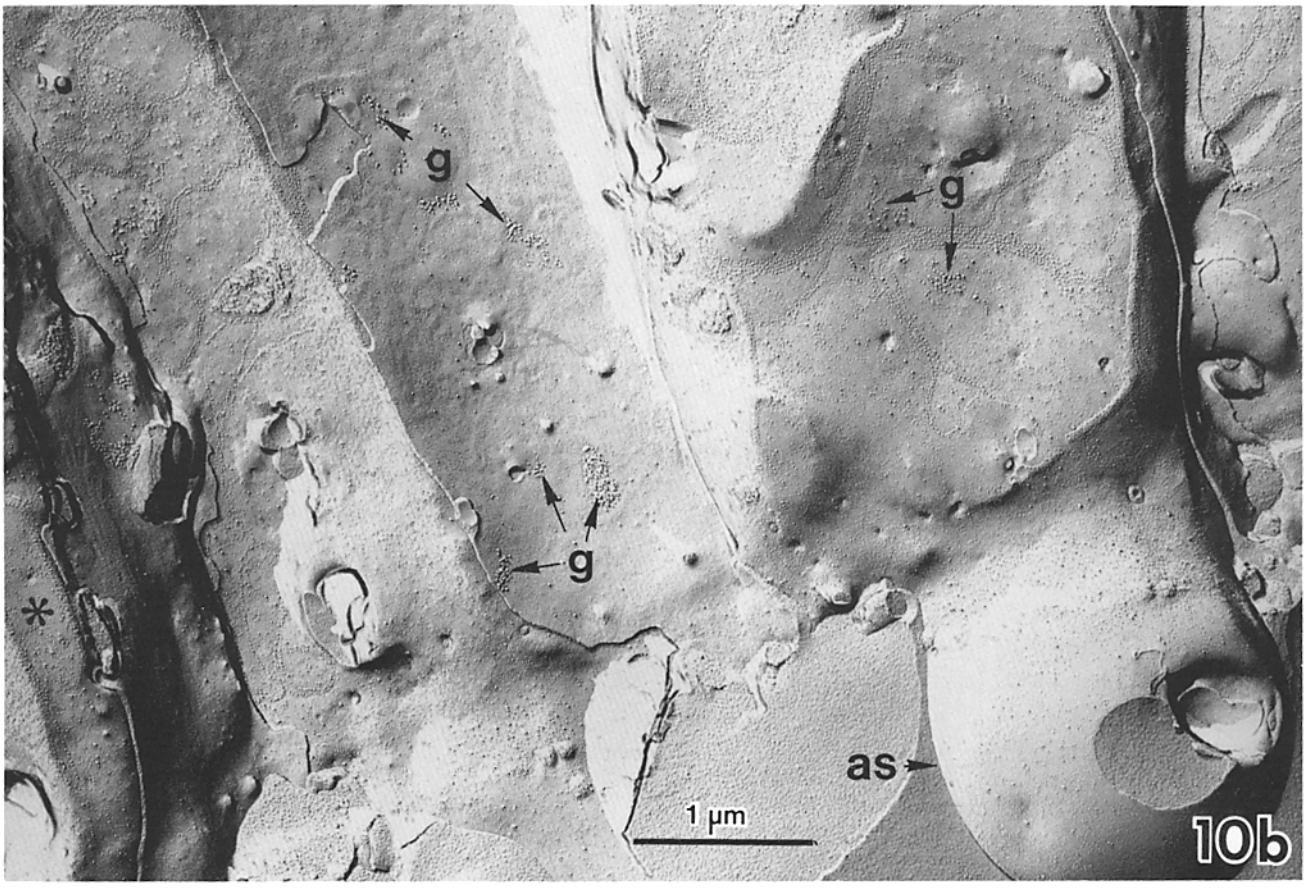
g
g
g
as
1 µm
10b

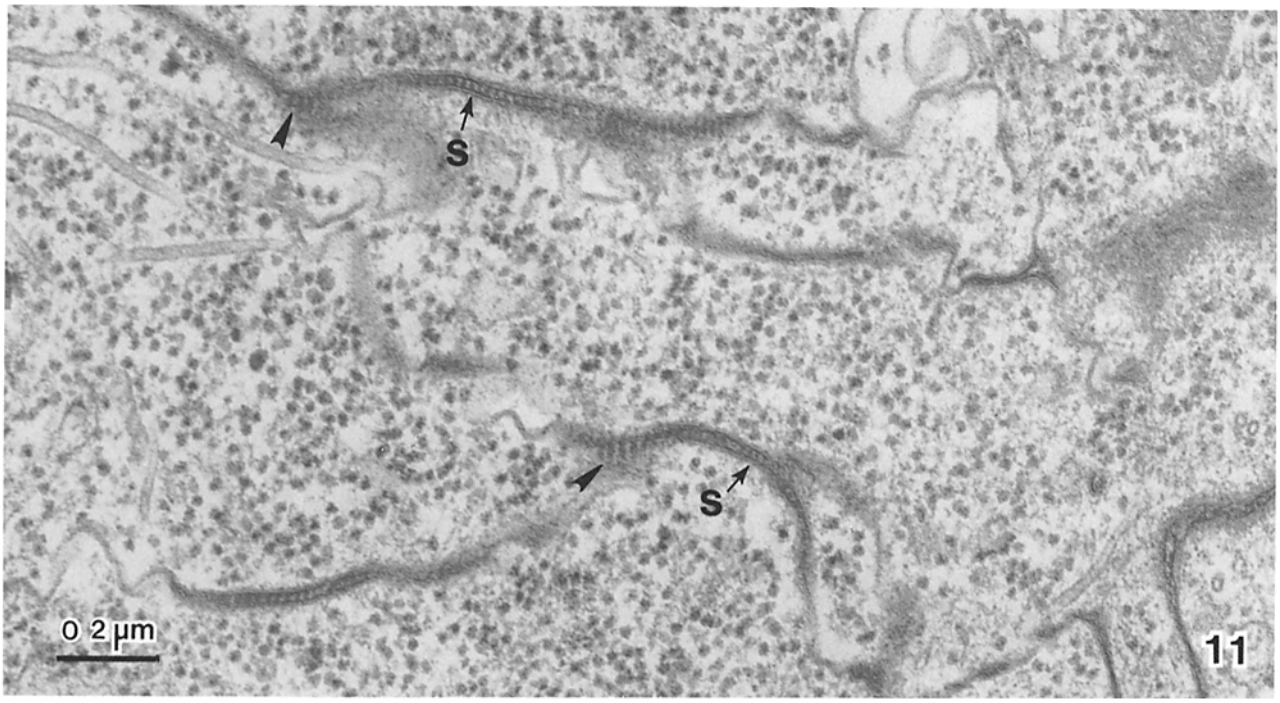

FIGURE 11 A thin section of a disk in which evagination was accelerated by 0.1% trypsin. Transversely sectioned septa (*s*) are evident and obliquely sectioned three-cell intersections show indications of tricellular plugs (arrows). × 65,000.

The redistribution of septa provides an attractive alternative to the continuous breakdown and re-formation of septa during cell rearrangement. One way in which exchange of neighbors can occur during cell rearrangement is shown in Fig. 12 as a process whereby one cell becomes inserted between two other cells. As cell *B* is inserted between cells *A* and *C*, the zone of contact between *B* and *C* increases, and that between *A* and *C* decreases. These areas of contact between adjacent cells are referred to as contact domains. It is proposed that as the width of a domain changes, the existing septa are redistributed in the plane of the membrane so that septa always stretch across the entire domain and turn downwards at its lateral boundaries, as shown schematically in Fig. 13. Thus, as a domain increases in width the paths followed by the septa become relatively straight or stretched out and, conversely, as a domain narrows, the septa becomes bunched or compacted. This process would require that the septate components be able to move freely in the plane of the membrane, and that the lateral regions of the septa remain associated with three-cell intersections (perhaps via connections with the tricellular plugs). A precedent for mobility of junctional components is seen in the dispersal and reaggregation of gap-junction particles (22, 23). The dispersed state occurs as cells become physically separate and the junctions are no longer functional. The mechanism of septate junction redistribution proposed here differs from gap junction dispersal in that the elements of the junction move as a functional unit, so that adjacent cells remain in contact and maintain the permeability barrier.

Although redistribution of septa readily explains how cells might adjust to changing areas of contact, we are still faced with the problem of what happens when cells eventually separate (e.g., cells *A* and *C* in Fig. 12). A point is presumably reached where the septa and tricellular plugs break down or at least detach from the plasma membrane of one cell to allow cells to separate. Conversely, the establishment of new cell contacts will require the formation of new septate elements. Rather than undergoing a complete breakdown and resynthesis during neighbor exchanges, junction components might first dissociate into subunits as cells separated and then reassemble at nearby sites of new cell contacts.

At present, the best evidence for the redistribution of septa is that in extensive observations of freeze-fractured and thin-sectioned disks, the septate junction has always appeared as described in the first half of this paper even when rapid cell rearrangements are occurring, i.e., there is no evidence for extensive turnover or dispersal and reassembly of septate junction components. This is in contrast to the gap junctions in trypsin-treated disks (Fig. 10*b*), in which varying degrees of dispersal of gap particles can be seen. It was also observed that where contact domains are broad the P-face particle rows tend to run parallel to the surface of the epithelium, whereas in narrow domains the particle rows are more circuitous and/or oriented predominantly vertically (e.g., in the narrow basal region of the *A/D* domain in Fig. 4).

Wherever a three-cell intersection can be unequivocally identified in freeze-fracture, the P-face rows of particles turn

FIGURE 10 Freeze-fracture micrographs of imaginal disks that have undergone accelerated evagination in the presence of 0.1% trypsin. (*a*) P-face particles (black arrows) are aligned along the three-cell intersection at left and E-face particles (white arrows) along the three-cell intersection at right. Asterisks indicate interdigitations between cells. × 60,000. (*b*) A low-power micrograph shows the typical distribution of septate particles over a number of adjacent cell surfaces. Gap junctions (*g*), in contrast, show varying degrees of particle dispersal. This may be an artifact induced by trypsinization or evidence for the dispersal and reaggregation of gap junctions associated with rapid cell rearrangement. × 24,000.

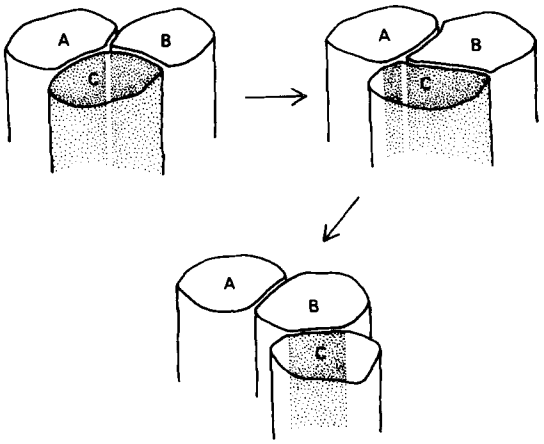

FIGURE 12 Schematic representation of the rearrangement of three cells, *A*, *B*, and *C*. Stippled areas indicate contact domains between pairs of adjacent cells. As cell *B* inserts between cells *A* and *C*, the *B/C* domain expands, and the *A/C* domain narrows and finally disappears.

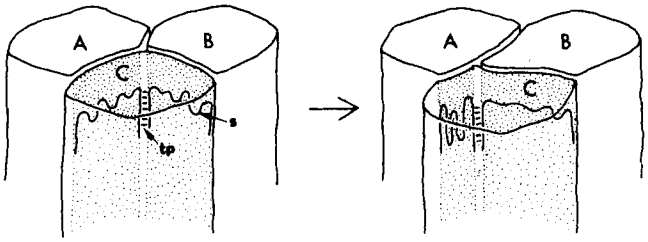

FIGURE 13 Scheme for the redistribution of septa during cell rearrangement. Septa (*s*) adjust to the changing width of a contact domain by becoming increasingly compacted (as in the *A/C* domain) or extended (as in the *B/C* domain). Lateral ends of the septa may be attached to the tricellular plug (*tp*).

down along the intersection but do not cross it. However, there are some regions which do not appear to be three-cell intersections where several P-face rows run vertically (small white asterisks in Figs. 4 and 5). Because these regions were only observed in evaginating disks they may in some cases represent the position of a three-cell intersection at a previous point in time. Finally, it is noted that in very narrow domains (e.g., between cells *A* and *B* in Fig. 7 and in the domain marked with an asterisk in Fig. 10*b*, only the most lateral septa, i.e., those immediately adjacent to the intersection, appear to be present, indicating that these lateral elements are the last to disappear in an old domain and/or the first to appear in a new one.

DISCUSSION

The recent review of septate and scalariform junctions by Noirot-Timothée and Noirot (15) includes a description of "tricellular" junctions in insect gut epithelia and provides the first evidence that the septate junction is not arranged as a continuous girdle around a cell. The arrangement of the septate junction in imaginal disks presented here agrees in all major respects with the observations of Noirot-Timothée and Noirot (15). Each cell is surrounded by a number of discrete septate domains equal to the number of neighboring cells. Each domain is crossed by long continuous stretches of septa separating the apical from the basal extracellular space and is closed laterally by the downturning of septa at three-cell intersections. The small channels left at three-cell intersections are filled with tricellular plugs of closely stacked diaphragms. Thus, the septate junction as a whole can function as a transepithelial barrier even though a single septum does not encircle the entire cell.

The presence of such an arrangement in both embryonic imaginal disk tissue and fully differentiated gut tissue suggests that this arrangement is a general one. Indeed, careful inspection of published micrographs of septate junctions support this idea. For example, micrographs of thin sections passing across three-cell intersections commonly show transversely sectioned septa near the intersection. Some clear examples include Fig. 7 in Hand and Gobel (24), Figs. 8 and 13 in Wood and Kuda (12), Fig. 3 in Caveney and Podgorski (25), and Fig. 20 in Poodry and Schneiderman (26). Micrographs of structures having the characteristics of the tricellular plugs described here and in reference 15 also appear in the literature, e.g., Fig. 7 in Leik and Kelly (27), Figs. 9 and 10 in Szollosi and Marcaillou (11), and Figs. 6–8, 13, and 14 in Baskin (28). In all three of these examples, the presence of longitudinally sectioned septa lying adjacent and at right angles to the diaphragms of the plug rules out the possibility that such structures represent transversely sectioned septa (see Fig. 8). Indeed, the micrographs of Baskin (28) provide the clearest high-resolution micrographs of tricellular plugs available to date. Finally, Fig. 5 in Wood (29) shows a freeze-fracture micrograph of septate particles closely following a three-cell intersection where adjacent cells interdigitate. These observations include representatives of three widely divergent invertebrate phyla (coelenterates, polychaetes, and arthropods), so it seems reasonable to conclude that the organization of the septate junction described here and by Noirot-Timothée and Noirot (15) is characteristic of most septate-containing tissues.

There are also some important parallels between septate and tight junction organization. It has been shown (30, 31) that at three-cell intersections the most apical sealing element of the tight junction turns downwards and runs parallel to the intersection, forming a tripartite junction (31). Thus, the sealing elements of the tight junction also seem to be confined to contact domains between pairs of adjacent cells. However, the lateral elements of the tripartite junction are in such close proximity that there is effectively no intercellular channel at three-cell intersections.

The flexibility of an arrangement where junctional components are confined to areas of contact between pairs of adjacent cells is evident in the model described here for the redistribution of septa during cell rearrangement. The model proposes that intact septa become extended or compacted in response to changes in the width of contact domains between cells. Some turnover or dispersal and reassembly of junctional elements is also required at the points of neighbor exchanges. This model provides, at least theoretically, for the maintenance of a permeability barrier during cell rearrangement, although the effectiveness of this barrier has not been measured in disks. However, a transepithelial barrier is apparently maintained by tight junctions during cell rearrangements in amphibian gastrulation (6). It will be of interest to learn whether the behavior of tight and septate junctions in other epithelia known to undergo cell rearrangement is similar to that of septate junctions in disks. As well as allowing cell rearrangement, redistribution of junction elements in the plane of the membrane also allows junctions to accommodate changes in cell shape. For example, as a cell expands its circumference, all its contact domains will expand, without necessarily altering the relative position of

three-cell intersections. Hull and Staehelin (32) have shown that loosely interconnected tight-junction networks in the intestinal epithelium of *Xenopus* tadpoles stretch out as the cells expand in diameter and become compressed as cells decrease in diameter. Pitelka and Taggart (manuscript in preparation) have also found that the tight-junction network in cultures of mammary epithelial cells alters its alignment and degree of compression in response to mechanical stress. Thus, it is possible that redistribution of intact, functioning components in both septate and tight junctions can occur in many tissues, providing a mechanism whereby the transepithelial barrier can be maintained during morphogenetic cell movements and cell shape changes.

Use of the Balzers 360M freeze-fracturing device and JEOL JEM 100CX electron microscope were kindly provided by the Electron Microscope Laboratory of the University of California, Berkeley. Special thanks are due to Dr. Janet Boyle for her unstinting assistance with all phases of the freeze-fracture procedures. Thanks also to Drs. Dorothy Pitelka, Raymond Keller, and James Fristrom for their valuable comments on the manuscript.

This work was supported by National Institutes of Health grant GM19937 to Dr. J. W. Fristrom.

Received for publication 15 December 1981, and in revised form 1 March 1982.

REFERENCES

1. Dipasquale, A. 1975. Locomotory activity of epithelial cells in culture. *Exp. Cell Res.* 94:191–215.
2. Trinkaus, J. P. 1976. On the mechanism of metazoan cell movements *In* The Cell Surface in Animal Embryogenesis and Development. G. Poste and G. L. Nicolson, editors. North Holland Publishing Co., Amsterdam. 225–329.
3. Fristrom, D., and J. W. Fristrom. 1975. The mechanism of evagination of imaginal discs of *Drosophila melanogaster*. I. General considerations. *Dev. Biol.* 43:1–23.
4. Fristrom, D. 1976. The mechanism of evagination of imaginal discs of *Drosophila melanogaster*. III. Evidence for cell rearrangement. *Dev. Biol.* 54:163–171.
5. Jacobson, A. G., and R. Gordon. 1976. Changes in the shape of the developing vertebrate nervous system analyzed experimentally, mathematically and by computer simulation. *J. Exp. Zool.* 191:197–246.
6. Keller, R. E. 1978. Time-lapse cinemicrographic analysis of superficial cell behavior during and prior to gastrulation. *J. Morphol.* 157:223–247.
7. Kageyama, T. 1982. Cellular basis of epiboly of the enveloping layer in the embryo of the medaka, *Oryzias latipes*. II. Evidence for cell rearrangement. *J. Exp. Zool.* 209:241–256.
8. Graf, L., and A. Gierer. 1980. Size, shape and orientation of cells in budding hydra and regulation of regeneration in cell aggregates. *Wilhelm Roux's Arch. Dev. Biol.* 188:141–151.
9. Fristrom, D. K., and W. L. Rickoll. Morphogenesis of imaginal discs of *Drosophila*. *In* Insect Ultrastructure, Vol. I. R. King and H. Akai, editors. Plenum Publishing Corp., New York. In press.
10. Staehelin, L. A. 1974. Structure and function of intercellular junctions. *Int. Rev. Cytol.* 39:191–283.
11. Szollosi, A., and C. Marcaillou. 1977. Electron microscope study of the blood-testis barrier in an insect: *Locusta migratoria*. *J. Ultrastruct. Res.* 59:158–172.
12. Wood, R. L., and A. M. Kuda. 1980. Formation of junctions in regenerating hydra: septate junctions. *J. Ultrastruct. Res.* 70:104–117.
13. Gilula, N. B., D. Branton, and P. Satir. 1970. The septate junction: a structural basis for intercellular coupling. *Proc. Natl. Acad. Sci. U. S. A.* 67:213–220.
14. Noirot-Timothée, C., D. S. Smith, M. L. Cayer, and C. Noirot. 1978. Septate junctions in insects: comparison between intercellular and intramembranous structures. *Tissue Cell.* 10:125–136.
15. Noirot-Timothée, C., and C. Noirot. 1980. Septate and scalariform junctions in arthropods. *Int. Rev. Cytol.* 63:97–140.
16. Eugene, O., M. A. Yund, and J. W. Fristrom. 1979. Preparative isolation and short-term organ culture of imaginal discs of *Drosophila melanogaster*. *In Tissue Culture Association Manual.* 5:1055–1062.
17. Robb, J. A. 1969. Maintenance of imaginal discs of *Drosophila melanogaster* in chemically defined media. *J. Cell Biol.* 41:876–884.
18. Fekete, É., D. Fristrom, I. Kiss, and J. W. Fristrom. 1975. The mechanism of evagination of imaginal discs of *Drosophila melanogaster*. II. Studies on trypsin-accelerated evagination. *Wilhelm Roux' Archiv. Entwicklungsmech. Org.* 178:123–138.
19. Fristrom, D., and C. Chihara. 1978. The mechanism of evagination of imaginal discs of *Drosophila melanogaster*. V. Evagination of disc fragments. *Dev. Biol.* 66:564–570.
20. Locke, M. 1965. The structure of septate desmosomes. *J. Cell Biol.* 25:166–168.
21. Branton, D., S. Bullivant, N. B. Gilula, M. J. Karnovsky, H. Moore, K. Mühlethaler, D. H. Northcote, L. Packer, B. Satir, P. Satir, V. Speth, L. A. Staehelin, R. L. Steere, and R. S. Weinstein. 1975. Freeze-etching nomenclature. *Science (Wash. D. C.)* 190:54–56.
22. Huebner, E., and H. Injeyan. 1981. Follicular modulation during oocyte development in an insect: formation and modification of septate and gap junctions. *Dev. Biol.* 83:101–113.
23. Lane, N. J., and L. S. Swales. 1980. Dispersal of junctional particles, not internalization, during the *in vivo* disappearance of gap junctions. *Cell.* 19:579–586.
24. Hand, A. R., and S. Gobel. 1972. The structural organization of the septate and gap junction of *Hydra*. *J. Cell Biol.* 52:397–408.
25. Caveney, S., and C. Podgorski. 1975. Intercellular communication in a positional field. Ultrastructrual correlates and tracer analysis of communication between insect epidermal cells. *Tissue Cell.* 7:559–574.
26. Poodry, C. A., and H. A. Schneiderman. 1971. Intercellular adhesivity and pupal morphogenesis in *Drosophila melanogaster*. *Wilhelm Roux' Archiv. Entwicklungsmech. Org.* 168:1–9.
27. Leik, J., and D. E. Kelly. 1970. Septate junctions in the gastrodermal epithelium of phialidium: a fine structural study utilizing ruthenium red. *Tissue Cell.* 2(3):435–441.
28. Baskin, D. G. 1977. The fine structure of polychaete septate junctions. *Cell Tissue Res.* 174:55–68.
29. Wood, R. L. 1977. The cell junction of hydra as viewed by freeze-fracture replication. *J. Ultrastruct. Res.* 58:299–315.
30. Friend, D. S., and N. B. Gilula. 1972. Variations in tight and gap junctions in mammalian tissues. *J. Cell Biol.* 53:758–776.
31. Staehelin, L. A. 1973. Further observations on the fine structure of freeze-cleaved tight junctions. *J. Cell Sci.* 13:763–786.
32. Hull, B., and L. A. Staehelin. 1976. Functional significance of the variations in the geometrical organization of tight junction networks. *J. Cell Biol.* 68:688–704.